

## **Author Manuscript**

**Title:** Molecular rotational correlation times and nanoviscosity determined by  $^{111}\text{mCd}$  perturbed angular correlation (PAC) of  $\gamma$ -rays spectroscopy

**Authors:** Rasmus Fromsejer; Marianne L. Jensen; Matthew O. Zacate; Victoria Karner; Vincent L. Pecoraro; Lars Hemmingsen

This is the author manuscript accepted for publication. It has not been through the copyediting, typesetting, pagination and proofreading process, which may lead to differences between this version and the Version of Record.

**To be cited as:** 10.1002/chem.202203084

**Link to VoR:** <https://doi.org/10.1002/chem.202203084>

# Molecular Rotational Correlation Times and Nanoviscosity Determined by $^{111}\text{mCd}$ Perturbed Angular Correlation (PAC) of $\gamma$ -rays Spectroscopy

Rasmus Fromsejer<sup>[a]</sup>, Marianne L. Jensen<sup>[b]</sup>, Matthew O. Zacate<sup>[c]</sup>, Victoria L. Karner<sup>[d]</sup>, Vincent L. Pecoraro<sup>[e]</sup>, Lars Hemmingsen<sup>[a]\*</sup>

[a] R. Fromsejer, Assoc. Prof. L. Hemmingsen  
Department of Chemistry  
University of Copenhagen  
Universitetsparken 5, 2100 København Ø, Denmark  
E-mail: lthe@chem.ku.dk

[b] M. L. Jensen  
Niels Bohr Institute  
University of Copenhagen  
Blegdamsvej 17, 2100 København Ø, Denmark

[c] Prof. M. O. Zacate  
Department of Physics, Geology, and Engineering Technology  
Northern Kentucky University  
Highland Heights, KY 41099-1900, USA

[d] Dr. V. L. Karner  
TRIUMF  
4004 Wesbrook Mall, Vancouver, BC, V6T 2A3, Canada

[e] Prof. V. L. Pecoraro  
Department of Chemistry, Willard H. Dow Laboratories  
University of Michigan  
930 N. University Ave., Ann Arbor, MI 48109-1055, USA

Supporting information for this article is given via a link at the end of the document.

**Abstract:** Nanoviscosity experienced by molecules in solution may be determined through measurement of the molecular rotational correlation time,  $\tau_c$ , e.g., by fluorescence and NMR spectroscopy. With this work, we apply PAC spectroscopy to determine the rate of rotational diffusion,  $\lambda=1/\tau_c$ , of a *de novo* designed protein, TRIL12AL16C, in solutions with viscosities,  $\xi$ , from 1.7 to 88 mPa·s. TRIL12AL16C was selected as molecular probe, because it exhibits minimal effects of intramolecular dynamics and static line broadening, allowing for exclusive elucidation of molecular rotation diffusion.  $\lambda$  determined by PAC spectroscopy agrees well with literature data from fluorescence and NMR spectroscopy, and scales linearly with  $1/\xi$  in agreement with the Stokes-Einstein-Debye model. PAC experiments require only trace amounts ( $\sim 10^{11}$ ) of probe nuclei and can be conducted over a broad range of sample temperatures and pressures. Moreover, most materials are relatively transparent to  $\gamma$ -rays. Thus, PAC spectroscopy may find applications under circumstances where conventional techniques cannot be applied, spanning from physics of liquids to *in vivo* biochemistry.

## Introduction

Diffusion controlled chemical and biochemical reaction rates are in part determined by the viscosity of the solvent, as are the mechanical properties of liquids. Thus, considerable effort has been devoted to experimental determination of viscosity. A family of techniques, including fluorescence and Nuclear Magnetic Resonance (NMR) spectroscopy,<sup>[1–5]</sup> rely on measuring rotational correlation times,  $\tau_c$ , and utilize the fact that  $\tau_c$  correlates with

viscosity. The simplest account of this correlation is given by the Stokes-Einstein-Debye relation:<sup>[6,7]</sup>

$$\tau_c^{SED} = \frac{V\xi}{kT} \quad (1)$$

where  $V$  is the effective molecular volume, typically including a hydration layer,  $\xi$  is the viscosity,  $k$  is Boltzmann's constant, and  $T$  the absolute temperature.

Perturbed angular correlation (PAC) spectroscopy is a nuclear physical technique, in which the angular correlation between two  $\gamma$ -rays emitted in succession from a radioactive probe is recorded as a function of time, with  $t = 0$  given by detection of the first  $\gamma$ .<sup>[8,9]</sup> Conservation of angular momentum in the nuclear decay gives rise to anisotropic emission of the second  $\gamma$ -rays with respect to the direction in which the first  $\gamma$ -ray is emitted, i.e.,  $\gamma$ - $\gamma$  angular correlation.<sup>[8,9]</sup> If the nucleus experiences extra-nuclear magnetic fields or electric field gradients (EFGs) during the time it is in the intermediate nuclear level (prior to emission of  $\gamma_2$ ), the angular correlation is perturbed. In the data presented here, the leading perturbation is the nuclear quadrupole interaction (NQI) between the nuclear electric quadrupole moment and the EFG originating from the surrounding charge distribution. Measuring the PAC of the  $\gamma$ -rays, allows for interrogation of the NQI at the probe site, reflecting the local molecular and electronic structure, as well as dynamics.<sup>[9]</sup> Dynamics may be due to local probe site dynamics as well as global molecular rotational diffusion.

For randomly oriented species, such as molecules in solution, the NQI may be characterized by two parameters,  $\omega_0$  and  $\eta$ ,

## RESEARCH ARTICLE

commonly referred to as the interaction strength and the asymmetry, respectively. For an intermediate state with nuclear spin  $I = 5/2$ , which is the case for several PAC isotopes including  $^{111m}\text{Cd}$ :<sup>[8,9]</sup>

$$\omega_0 = \frac{12\pi|V_{zz}eQ|}{40h} \quad (2)$$

$$\eta = \frac{V_{xx} - V_{yy}}{V_{zz}} \quad (3)$$

Where  $V_i$  are the diagonal elements of the EFG tensor in the principal axis system, ordered such that  $|V_{xx}| \leq |V_{yy}| \leq |V_{zz}|$ ,  $e$  is the charge of the electron,  $Q$  is the nuclear electric quadrupole moment and  $h$  is Planck's constant.

For time independent NQIs and randomly oriented species, the perturbation function for  $I=5/2$  is:<sup>[9,10]</sup>

$$G_{22}^{static}(t) = a_0 + a_1 \cos(\omega_1 t) + a_2 \cos(\omega_2 t) + a_3 \cos(\omega_3 t) \quad (4)$$

where  $a_i$  and  $\omega_i$  depend on  $\omega_0$  and  $\eta$  of the NQI. The  $I = 5/2$  intermediate nuclear level is split into three sublevels due to the NQI, and  $\omega_i$  directly reflect the energy differences ( $\hbar\omega_i$ ) of these sublevels. Thus  $\omega_3 = \omega_1 + \omega_2$ , which is of course obeyed by the three frequencies in Figure 1B. Moreover, a Lorentzian line shape is often applied, with the parameter  $\delta$  accounting for the so-called static line broadening.

The effect of stochastic time dependent NQIs, for example due to molecular rotational diffusion, on PAC spectra is divided into the slow or fast dynamics time regimes, with the time scale determined by  $\omega_0$ . For slow rotational diffusion ( $\omega_0\tau_c \gg 1$ ), the static perturbation function, equation (4), becomes exponentially damped:<sup>[9,10]</sup>

$$G_{22}^{slow\ rotational\ diffusion}(t) = e^{-\lambda t} G_{22}^{static}(t) \quad (5)$$

where  $\lambda$  is the rate of the dynamic process, which for pure rotational diffusion is  $\lambda = 1/\tau_c$ .

For rapid rotational diffusion ( $\omega_0\tau_c \ll 1$ ), the perturbation function becomes an exponentially decaying function without oscillatory behaviour:<sup>[8,9]</sup>

$$G_{22}^{fast\ rotational\ diffusion}(t) = e^{-2.8\frac{\omega_0^2}{\lambda}(1+\frac{\eta^2}{3})t} \quad (6)$$

Note that the  $\lambda (= 1/\tau_c)$  used here, should not be confused with the  $\lambda$ , often used in PAC literature in the fast dynamics time regime.

Several past PAC studies have reported the effect of dynamics on the spectroscopic signal.<sup>[9-21]</sup> However, the molecular motion comprises both global rotational diffusion and local intramolecular dynamics, and thus, in most cases, the effective, combined dynamics of the molecule were observed.

With this work we selected the *de novo* designed protein, TRIL12AL16C, which belongs to a family of peptides forming coiled coils, as molecular probe. The mother TRI peptide is composed of 4 heptad repeats with glycines at the N- and C-termini, Ac-G(LKALEEK)<sub>4</sub>G-NH<sub>2</sub>. TRIL12AL16C has substitutions

at positions 12 (L12A) and 16 (L16C), and forms a trimeric coiled coil under the experimental conditions used here. The Cd<sup>II</sup> binding site is composed of three thiolate (cysteinate) ligands and a water molecule, i.e., CdS<sub>3</sub>O.<sup>[22]</sup> This protein displays a very well-defined metal site with narrow lines in the  $^{111m}\text{Cd}$  PAC spectrum, demonstrating that static line broadening as well as the effect of intramolecular dynamics on the PAC signal is minimal.<sup>[23]</sup> This makes TRIL12AL16C an ideal model system to study the effect of global molecular rotational diffusion on the PAC signal. More specifically, the rotational correlation time may be recorded by  $^{111m}\text{Cd}$  PAC spectroscopy in the slow reorientation time regime, thereby allowing for determination of the nanoviscosity experienced by the protein. Such PAC probe – molecule complexes may be designed for direct determination of rotational correlation times and nanoviscosity in a variety of settings from physics to biochemistry.

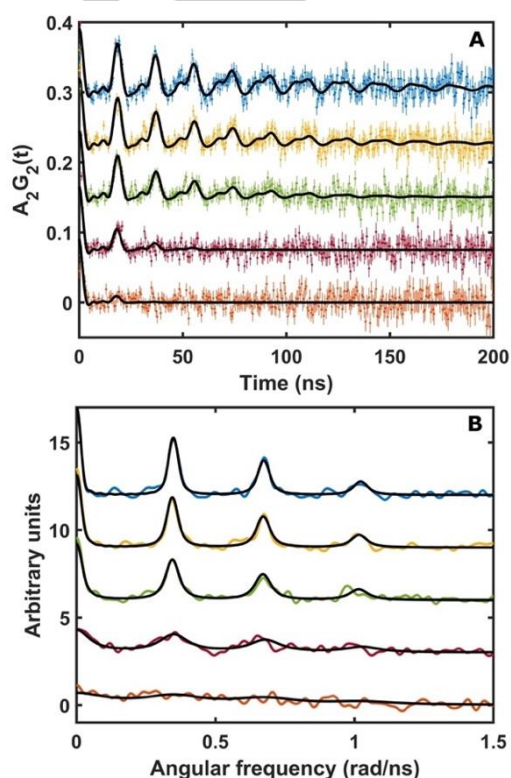


**Figure 1.**  $^{111m}\text{Cd}$  PAC data (A) and Fourier transformed data (B, data indicated as a coloured line and fit as a black line) for the *de novo* designed protein, TRIL12AL16C, recorded at 1 °C and various viscosities. The viscosities decrease from top to bottom: 88, 29, 9.8, 3.4, 1.7 mPa·s.

## Results and Discussion

The experimental conditions and the parameters obtained from fitting the PAC data are presented in Table 1 and the corresponding PAC spectra are presented in Figure 1. Sucrose was added to the solutions to control the viscosity. For additional details on the PAC measurements and fitting, see the Experimental section and the Supporting Information.

**Table 1.** Fit parameters for the  $^{111}\text{mCd}$  PAC data for the model protein, TRIL12AL16C (at 1 °C and various viscosities,  $\xi$ ), and calculated  $\lambda_{\text{SED}}$  and  $\tau_{\text{c}}^{\text{SED}}$  within the Stokes-Einstein-Debye approximation, see Equation (1) and Figure 1. Error bars on the PAC parameters are statistical standard deviations based on the fit to the data. Error bars on the calculated  $\lambda_{\text{SED}}$  and  $\tau_{\text{c}}^{\text{SED}}$  are determined assuming that the error bar on the temperature is  $\pm 1$  °C, and the error bar on the sucrose concentration is  $\pm 1\%$  w/w. f: fixed in the fit. A is the amplitude of the signal, and the remaining parameters are described in the text.

Sucrose	$\xi$	$\omega_0$	$\eta$	$\delta$	A	$\lambda_{\text{exp}}$	$\tau_{\text{c}}^{\text{exp}}$	$\lambda_{\text{SED}}$	$\tau_{\text{c}}^{\text{SED}}$
% w/w	mPa·s	Mrad/s		×100	×100	$\mu\text{s}^{-1}$	ns	$\mu\text{s}^{-1}$	ns
55	88(15)	340.4(3)	0.143(4)	1.4(1)	9.3(2)	3.22(40)	310(39)	1.96(33)	511(87)
55	88(15)	343.6(5)	0.161(5)	2.0(2)	8.3(3)	3.83(55)	261(37)	1.96(33)	511(87)
55	88(15)	338.7(8)	0.16(1)	1.9(4)	9.3(5)	5.9(1.2)	169(34)	1.96(33)	511(87)
47	29(3.5)	337(1)	0.14(1)	1.8f	9.7(5)	10.7(1.4)	93(12)	5.94(72)	168(20)
36	9.8(0.8)	337(1)	0.15(2)	1.8f	9.7(6)	17.2(2.1)	58.1(7.1)	17.6(1.4)	56.9(4.6)
19	3.5(0.3)	340.9f	0.155f	1.8f	9.3f	52.9(5.2)	18.9(1.9)	49.2(4.2)	20.3(1.7)
0	1.7(0.1)	340.9f	0.155f	1.8f	9.3f	118(21)	8.5(1.5)	101(6.0)	9.86(58)

As expected, an oscillating PAC signal is observed within the slow dynamics time regime ( $\omega_0\tau_{\text{c}} \gg 1$ ) for the experiment with high viscosity,<sup>[23]</sup> Figure 1A ( $\xi = 88$  mPa·S). Damping of the signal increases with decreasing viscosity, leading to essentially complete damping for the experiment with lowest viscosity, Figure 1A ( $\xi = 1.7$  mPa·S). The three frequencies of the well-defined NQI can be seen readily in Fourier transforms of perturbation functions, Figure 1B, with linewidth that increases with decreasing viscosity. There are two contributions to the linewidth, the static line broadening represented by the parameter  $\delta$ , and the dynamic line broadening represented by  $\lambda$ . The two parameters differ in how they affect data: The signal at zero frequency, i.e., the  $a_0$  term of the perturbation function, see equation (4), is only affected by dynamic line broadening and not by static line broadening. In contrast, the other three terms of the perturbation function are affected by both types of line broadening. The dynamic line broadening is therefore directly observable by the broadening and decreased intensity of the signal at zero frequency, see Figure 1B. Moreover, the static line broadening is expected to be almost constant throughout the series of experiments (because the metal site is embedded within the protein) and can therefore not account for the progressive increase of the line broadening with decrease of viscosity.

In Figure 2A, the values of  $\lambda_{\text{exp}}$  obtained from the  $^{111}\text{mCd}$  PAC experiments are plotted against  $\lambda_{\text{SED}}$ , calculated within the Stokes-Einstein-Debye approximation, along with data for various proteins determined using fluorescence and NMR spectroscopy.<sup>[1,2]</sup> The PAC data presented here compare well with the data from the literature, validating the use of this method to measure rotational diffusion.

In Figure 2B, a linear fit of  $\lambda_{\text{exp}}$  against  $\lambda_{\text{SED}}$  is presented for the PAC data. The measured rate of dynamics is composed of two contributions, the global rotational diffusion and intramolecular dynamics of the protein affecting the metal site, as described by  $\lambda_{\text{exp}} = a \cdot \lambda_{\text{SED}} + \lambda_{\text{intramolecular}}$ , assuming that the global rotational diffusion rate is proportional to  $T/(V\xi)$ , and that the intramolecular

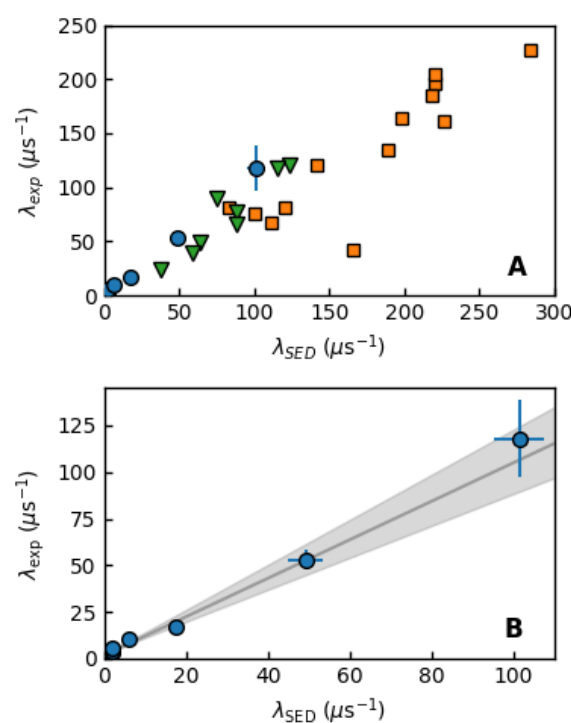


**Figure 2.** Experimental data for the characteristic rate of dynamics,  $\lambda_{\text{exp}}$ , versus the theoretical reciprocal rotational correlation time within the Stokes-Einstein-Debye model,  $\lambda_{\text{SED}}$  ( $=1/\tau_{\text{c}}$ ) for the TRIL12AL16C protein. A:  $^{111}\text{mCd}$  PAC data (blue data points with error bars) compared to fluorescence (green inverted triangles) and NMR (orange squares) spectroscopic data.<sup>[1,2]</sup> B:  $^{111}\text{mCd}$  PAC data points with a line of best fit (the data point with the largest value of  $\lambda$  was not included in the fit because it does not fulfil  $\omega_0\tau_{\text{c}} \gg 1$ ):  $\lambda_{\text{exp}} = 1.0(1)\lambda_{\text{SED}} + 1.8(5) \mu\text{s}^{-1}$ . Note that the shaded area corresponds to points within one standard deviation of the fitted line.

dynamics is independent of the viscosity. This leads to  $\lambda_{\text{intramolecular}} = 1.8(5) \mu\text{s}^{-1}$ , which is a very small number, and corroborates the conclusion based on the narrow line width of the PAC signal, that

## RESEARCH ARTICLE

the metal site in TRIL12AL16C is relatively rigid. Using the data in Figure 2, a standard curve may be created, see Figure S2. For a given value of  $\lambda$  derived from a  $^{111}\text{mCd}$  PAC experiment for the reference molecule TRIL12AL16C, this standard curve allows for determination of the solvent viscosity.

Taken together, the systematic correlation of the PAC data with viscosity presented in Figure 1, Figure 2, Figure S2, and Table 1, and the comparison with data from the other spectroscopic techniques, indicates that PAC spectroscopy may be applied to reliably determine  $\lambda$  over the range of almost two orders of magnitudes of viscosity (1.7 – 88 mPa-s).

PAC spectroscopy provides access to a range of measurable correlation times, and here we estimate the limits. Lower and upper limits of  $\lambda$  depend on PAC isotope and strength of the NQI interaction (see supporting information for more detail). The lower limit (slow rotational diffusion) is controlled by the longest time (between the two  $\gamma$ -rays), for which good experimental S/N can be achieved, and therefore mainly by the lifetime of the intermediate nuclear level. For  $^{111}\text{mCd}$  the lower limit is on the order of  $\lambda = 1 \mu\text{s}^{-1}$ . For other PAC isotopes, e.g.,  $^{204}\text{mPb}$ , which has a longer intermediate state half-life, this limit might be decreased by a factor of about 3. The upper limit within the slow dynamics time regime is controlled by the requirement that  $\omega_0 \gg \lambda$ , i.e., by the measured frequency,  $\omega_0$ . For  $^{111}\text{mCd}$  PAC this leads to an upper limit of  $\lambda$  on the order of  $100 \mu\text{s}^{-1}$ . For other PAC isotopes, e.g.,  $^{181}\text{Hf}$  or  $^{199\text{m}}\text{Hg}$ , which often display larger  $\omega_0$ , this limit might be increased by a factor of about 3. In the fast dynamics time regime,  $\omega_0 \ll \lambda$ , however, the upper limit may be extended significantly, allowing for studies of molecular reorientation in the gas phase. The first PAC experiments on molecules in the gas phase were realized very recently, and indeed rapid reorientation was observed for  $^{199\text{m}}\text{HgI}_2$  in 1.8 bar of Ar at 300 °C due to collisions of  $\text{HgI}_2$  with the Ar gas molecules.<sup>[24]</sup>

The main advantages of PAC spectroscopy are: 1) Very low concentrations (pM-nM) of probe – molecule complex are required, because it is a radioisotope based technique, 2) Most materials are relatively transparent to  $\gamma$ -rays, allowing for experiments under conditions where visible light (fluorescence spectroscopy) cannot be applied, 3) The PAC instrument is mechanically stable and a broad range of temperatures, pressures, viscosities, etc. may be probed, 4) The dynamic range in which PAC spectroscopy is sensitive to changes of viscosities (or molecular rotational correlation times) spans almost 4 orders of magnitude, see Figure S1. Limitations of PAC spectroscopy include: 1) the experiments are relatively expensive and time consuming, 2) production of suitable radioisotopes is not trivial in most cases, and for short lived nuclei requires a production facility nearby, 3) PAC instruments are not commercially available. For a more elaborate overview of PAC spectroscopy, we refer the reader to the literature.<sup>[8,9]</sup>

Applications of PAC spectroscopy that may be envisioned using designed molecular nanosensors of viscosity include measurements of: The effects of confinement on the liquid's properties, rotational diffusion of (bio)molecules in various environments, molecular self-assembly/aggregate sizes and the concomitant changes in rotational correlation time, the process of

nanocrystallisation, and the determination of local microscopic viscosity. More generally in a physics perspective, change of dynamics of liquids upon change of temperature, pressure, or other experimental conditions may be explored. Moreover, pharmaceutical applications may include the fate of a labelled molecule *in vivo* by recording changes in rotational correlation times, e.g., for a labelled drug binding to a receptor. Similarly, for a probe initially trapped within a drug delivery agent such as a lipid vesicle, the lifetime of the vesicle may be monitored, because the probe will change rotational correlation time upon release from the vesicle as demonstrated about 40 years ago using time integrated PAC.<sup>[18–21]</sup>

## Conclusion

With this work, we have demonstrated that through careful selection of a PAC probe – molecule complex (here, the rigid Cd(II) binding site of the TRIL12AL16C protein), it is possible to directly determine the rate of molecular rotational diffusion,  $\lambda$ , over almost two orders of magnitude ( $3.2 - 118 \mu\text{s}^{-1}$ ). Using  $\lambda$ , we can estimate the viscosity, i.e., the nanoviscosity experienced by the tumbling protein. The experimentally determined  $\lambda$  values agree well with those determined by NMR and fluorescence spectroscopy on other proteins, corroborating our conclusion. Several applications of PAC spectroscopy may be envisioned from physics of liquids to *in vivo* biochemistry.

## Experimental

**Peptide synthesis and purification.** The protein TRIL12AL16C was prepared and characterized as described in Reference [23].

**PAC spectroscopy.** A six-detector PAC setup<sup>[25]</sup> with  $\text{BaF}_2$  detectors was used for the spectroscopic measurements. The time resolution was 0.86 ns, and the time-per-channel was 0.562 ns. Data analysis was carried out with the Winfit program (provided by Prof. T. Butz) using 700 data points excluding the first 2 points due to systematic errors near  $t = 0$ . Fourier transformation of the data and fits was carried out using 600 points after mirroring 300 data points and with a Keiser-Bessel parameter of 4. A Lorentzian line shape was used with the parameter  $\delta$  accounting for line broadening due to a static distribution of electric field gradients (EFGs). The experimental equivalent of  $G_{22}(t)$  to which the NQI parameters are fitted is:

$$R(t) = 2 \frac{W(180^\circ, t) - W(90^\circ, t)}{W(180^\circ, t) + 2W(90^\circ, t)} \quad (7)$$

where  $W(180^\circ, t)$  and  $W(90^\circ, t)$  are the geometrical mean of coincidence spectra recorded with  $180^\circ$  and  $90^\circ$  between detectors, after adjustment to the same ( $t=0$ ) start channel and baseline correction for random coincidences. As the information content of the experimental data gradually decreases with more damping (lower viscosity), see Table 1, it was necessary to fix parameters in the fit. First, the parameter reflecting local time-independent (on a time scale of a few hundreds of nanoseconds) variations from one molecule to the next,  $\delta$ , correlates with  $\lambda$ , and therefore  $\delta$  was fixed to the average value determined at the highest viscosity. Next, for the two experiments where the oscillating signal was strongly damped (viscosity of 1.7 and 3.4 mPa-s),  $\omega_0$  and  $\eta$  were fixed, and finally the amplitude was fixed for the experiment with viscosity of 1.7 mPa-s.

## RESEARCH ARTICLE

In Figure 1, the data for  $R(t)$  were shifted to have a base line at zero, and the Fourier transform was performed on these data (this does not affect the fitted parameters presented in Table 1).

The radioactive  $^{111m}\text{Cd}$  was produced at the University Hospital in Copenhagen and separated from  $^{108}\text{Pd}$  as described previously.<sup>[26]</sup> In a typical experiment, a small volume ( $\sim 10\ \mu\text{L}$ ) of  $^{111m}\text{Cd}$  in water was mixed with non-radioactive cadmium acetate, TRIS buffer, and TRIL12AL16C (in  $1\ \text{mM}\ \text{H}_2\text{SO}_4$ ), pH was adjusted to 7.9 at room temperature (and thus pH 8.5 at  $1\ ^\circ\text{C}$ , given the temperature dependence of the  $pK_a$  of TRIS), the sample was left for 10 min, and sucrose added to the desired concentration, thereby achieving final concentrations of  $300\ \mu\text{M}$  TRIL12AL16C (and thus  $100\ \mu\text{M}$  of the protein trimer),  $25\ \mu\text{M}\ \text{Cd}^{II}$ , and  $14\ \text{mM}$  TRIS in a final volume of  $\sim 100\ \mu\text{L}$ . pH was measured again after the PAC experiments and was in all cases  $8.4 \pm 0.2$  at  $1\ ^\circ\text{C}$ .

**Calculation of the rotational correlation time** for the molecule to which the PAC probe is bound was carried out within the Stokes-Einstein-Debye approximation for a spherical molecule:<sup>[6,7]</sup>

$$\tau_c^{SED} = \frac{V\xi}{kT} = \frac{4\pi(r_m + r_h)^3\xi}{3kT} \quad (8)$$

where  $V$  is effective molecular volume,  $r_m$  and  $r_h$  are the molecular radius and radius of hydration, respectively,  $\xi$  is the viscosity and  $T$  the absolute temperature.  $r_h = 3\ \text{\AA}$  was selected as is common practice, and  $r_m$  was determined by:

$$r_m = \left( \frac{3M}{4\pi\rho N_A} \right)^{1/3} \quad (9)$$

where  $M$  is the molecular mass,  $\rho$  is the density of the molecule set to  $1.37\ \text{g/cm}^3$ ,<sup>[27]</sup> and  $N_A$  is Avogadro's number.

The rate of rotational diffusion,  $\lambda_{SED}$ , which is closely related to the diffusion coefficient,  $D$  ( $\lambda_{SED} = 6D$ ), is calculated as:

$$\lambda_{SED} = \frac{1}{\tau_c^{SED}} \quad (10)$$

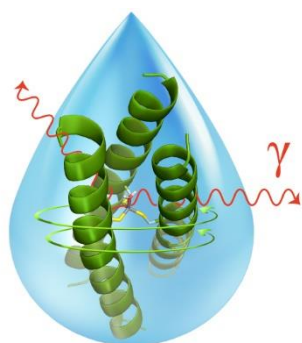
## Acknowledgements

The research leading to these results has received funding from the Danish Ministry of Higher Education and Science (NICE grant).

**Keywords:** Designed protein • PAC spectroscopy • Proteins • Rotational diffusion • Viscosity

- [1] J. García de la Torre, M. L. Huertas, B. Carrasco, *J. Magn. Reson.* **2000**, *147*, 138–146.  
 [2] J. R. Lakowicz, *Principles of Fluorescence Spectroscopy*, Springer, New York, **2006**.  
 [3] C. E. Cobb, E. J. Hustedt, J. M. Beechem, A. H. Beth, *Biophys. J.* **1993**, *64*, 605–613.  
 [4] A. Loman, I. Gregor, C. Stutz, M. Mund, J. Enderlein, *Photochem. Photobiol. Sci.* **2010**, *9*, 627–636.  
 [5] Y. Zhang, X. Wu, Y. Wang, S. Zhu, B. Z. Gao, X.-C. Yuan, *Laser Phys.* **2014**, *24*, 065601.  
 [6] F. Perrin, *J. Phys. Radium* **1934**, *5*, 497–511.  
 [7] D. Lavalette, C. Tétreau, M. Tourbez, Y. Blouquit, *Biophys. J.* **1999**, *76*, 2744–2751.  
 [8] H. Frauenfelder, R. M. Steffen, S. R. de Groot, H. A. Tollhoek, W. J. Huiskamp, in *Alpha-, Beta- and Gamma-Ray Spectroscopy* (Ed.: K. Siegbahn), North Holland, **1965**, pp. 997–1198.

- [9] L. Hemmingsen, K. N. Sas, E. Danielsen, *Chem. Rev.* **2004**, *104*, 4027–4062.  
 [10] E. Danielsen, R. Bauer, *Hyperfine Interact.* **1991**, *62*, 311–324.  
 [11] R. Bauer, A. Atke, E. Danielsen, J. Marcussen, C. E. Olsen, J. Rehfeld, T. Saermark, D. Schneider, H. Vilhardt, M. Zeppezauer, *Int. J. Radiat. Appl. Instrum. Part A* **1991**, *42*, 1015–1023.  
 [12] E. Danielsen, R. Bauer, D. Schneider, *Eur. Biophys. J.* **1991**, *20*, 193–201.  
 [13] T. Butz, A. Lerf, R. Huber, *Phys. Rev. Lett.* **1982**, *48*, 890–893.  
 [14] C. A. Kalfas, E. G. Sideris, S. El-Kateb, P. W. Martin, U. Kuhnlein, *Chem. Phys. Lett.* **1980**, *73*, 311–314.  
 [15] M. Stachura, S. Chakraborty, A. Gottberg, L. Ruckthong, V. L. Pecoraro, L. Hemmingsen, *J. Am. Chem. Soc.* **2017**, *139*, 79–82.  
 [16] F. J. Schwab, H. Appel, M. Neu, W.-G. Thies, *Eur. Biophys. J.* **1992**, *21*, 147–154.  
 [17] R. Fromsejer, L. Hemmingsen, *Hyperfine Interact.* **2019**, *240*, 88.  
 [18] K. J. Hwang, M. R. Mauk, *Proc. Natl. Acad. Sci. U. S. A.* **1977**, *74*, 4991–4995.  
 [19] M. R. Mauk, R. C. Gamble, J. D. Baldeschwieler, *Science* **1980**, *207*, 309–311.  
 [20] J. T. Derksen, J. D. Baldeschwieler, G. L. Scherphof, *Proc. Natl. Acad. Sci. U. S. A.* **1988**, *85*, 9768–9772.  
 [21] F. H. Roerdink, J. Regts, T. Handel, S. M. Sullivan, J. D. Baldeschwieler, G. L. Scherphof, *Biochim. Biophys. Acta, Biomembr.* **1989**, *980*, 234–240.  
 [22] O. Iranzo, T. Jakusch, K.-H. Lee, L. Hemmingsen, V. L. Pecoraro, *Chem. Eur. J.* **2009**, *15*, 3761–3772.  
 [23] K.-H. Lee, C. Cabello, L. Hemmingsen, E. N. G. Marsh, V. L. Pecoraro, *Angew. Chem. Int. Ed.* **2006**, *45*, 2864–2868.  
 [24] H. Haas, J. Röder, J. G. Correia, J. Schell, A. S. Fenta, R. Vianden, E. M. H. Larsen, P. A. Aggelund, R. Fromsejer, L. B. S. Hemmingsen, S. P. A. Sauer, D. C. Lupascu, V. S. Amaral, *Phys. Rev. Lett.* **2021**, *126*, 103001.  
 [25] T. Butz, S. Saibene, Th. Fraenzke, M. Weber, *Nucl. Instrum. Methods Phys. Res., Sect. A* **1989**, *284*, 417–421.  
 [26] L. Hemmingsen, R. Bauer, M. J. Bjerrum, M. Zeppezauer, H.-W. Adolph, G. Formicka, E. Cedergren-Zeppezauer, *Biochemistry* **1995**, *34*, 7145–7153.  
 [27] P. G. Squire, M. E. Himmel, *Arch. Biochem. Biophys.* **1979**, *196*, 165–177.



Brownian molecular tumbling rates in solution are measured using  $^{111}\text{mCd}$  perturbed angular correlation of  $\gamma$ -rays (PAC) spectroscopy and a *de novo* designed molecular probe (a trimeric coiled coil protein). Most materials are relatively transparent to  $\gamma$ -rays, and PAC spectroscopy may find applications where conventional methods probing rotational correlation times, e.g., NMR and fluorescence spectroscopy, cannot be applied - from physics of liquids to *in vivo* biochemistry.